Japan Antibiotics
Research Association

The Society for
Actinomycetes Japan

ARTICLE

Check for
updates

Bisprenyl naphthoquinone and chlorinated calcimycin congener bearing thiazole ring from an actinomycete of the genus *Phytohabitans*

Enjuro Harunari [1] · Shunsuke Mae[1] · Keisuke Fukaya[1] · Etsu Tashiro [2] · Daisuke Urabe[1] · Yasuhiro Igarashi [1]

Abstract

A bisprenyl naphthoquinone, phytohabinone (**1**), and a calcimycin congener with unusual modifications, phytohabimicin (**2**), were isolated from the culture extract of *Phytohabitans* sp. RD003013. The structures of **1** and **2** were determined by NMR and MS analyses, and the absolute configuration of **2** was established by using electronic circular dichroism (ECD) calculation. The prenylation pattern of **1** was unprecedented among the known prenylated naphthoquinones. Compound **2** represents a spiroacetal core of polyketide origin substituted with a thiazole carboxylic acid and a dichrolopyrrole moiety, which is an unprecedented modification pattern in the known calcimycin family natural products. Remarkably, **2** showed moderate antimicrobial activity against a Gram-negative bacterium *Ralstonia solanacearum* while calcimycin was inactive. Additionally, **2** inhibits the migration of EC17 cancer cells at noncytotoxic concentrations.

Introduction

Actinomycetes, especially filamentously growing groups such as *Streptomyces* and *Micromonospora*, are excellent producers of various natural products with remarkable bioactivities. However, discovery of new compounds from typical terrestrial actinomycetes is currently getting difficult, while a substantial number of actinomycetal genera are likely unstudied for their secondary metabolites. Rare actinobacteria that are less frequently isolated are now recognized as a promising reservoir of new natural products [1–3]. The genus *Phytohabitans* is a member of the family *Micromonosporaceae*, first described in 2010 [4] and until recently, habiterpenol was the only one known compound

from this genus [5]. Meanwhile, the latest genomic study indicated the presence of type I and III polyketides synthases (PKSs), nonribosomal peptide synthetase (NRPS), and hybrid PKS/NRPS gene clusters in the genome of *Phytohabitans* strains though the isolation of polyketides or peptidic compounds were not reported [6].

During the course of metabolite profiling in underexplored rare actinomycetes, we recently discovered new δ-lactone-terminated linear polyketides, phytohabitols, from *Phytohabitans* sp. RD002984 (Fig. 1) [7]. In this study, *Phytohabitans* sp. RD003013 isolated from a soil collected in Tokyo, Japan, was found to produce a bisprenyl naphthoquinone designated phytohabinone (**1**) and a calcimycin-class polyketide modified with a dichrolopyrrol and a thiazolecarboxylic acid designated phytohabimicin (**2**). We herein describe the isolation and structure elucidation of **1** and **2** along with their bioactivities.
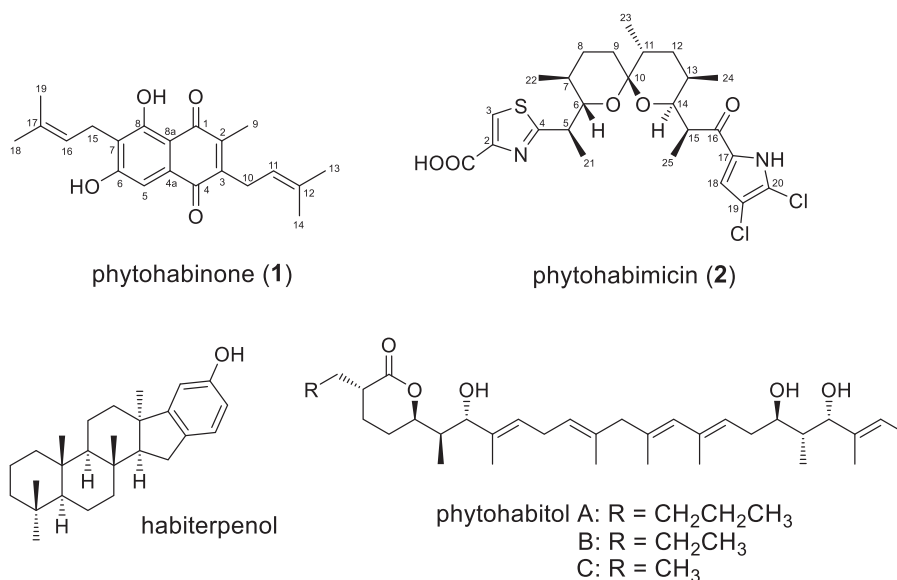
✉ Yasuhiro Igarashi
yas@pu-toyama.ac.jp

1 Biotechnology Research Center and Department of Biotechnology, Toyama Prefectural University, 5180 Kurokawa, Imizu, Toyama 939-0398, Japan

2 Showa Pharmaceutical University, 3-3165 Higashi-Tamagawagakuen, Machida, Tokyo 194-8543, Japan

Results and discussion

Phytohabinone (**1**) was isolated as a yellow amorphous solid (2.1 mg from 1 l of culture). HRESITOFMS gave a deprotonated molecular ion at *m/z* 339.1600, which defined a molecular formula $C_{21}H_{24}O_4$. The ^{1}H NMR spectrum of **1** revealed the presence of one aromatic singlet at δ_H 7.05, two olefinic triplets at δ_H 5.15 and 4.96, two methylene doublets

Fig. 1 Natural products from *Phytohabitans*

phytohabinone (**1**)

phytohabimicin (**2**)

habiterpenol

phytohabitol A: R = CH$_2$CH$_2$CH$_3$
B: R = CH$_2$CH$_3$
C: R = CH$_3$

at δ_H 3.26 and 3.23, five methyl singlets at δ_H 2.07, 1.72, 1.72, 1.64, and 1.62, one hydrogen-bonded hydroxy proton at δ_H 12.64, one phenolic hydroxy proton at δ_H 11.05. The ^{13}C and HSQC spectral data allowed the assignment of 21 carbons to two carbonyls at δ_C 188.4 and 183.2, two oxygenated sp^2 carbons at δ_C 161.7 and 160.8, seven sp^2 carbons at δ_C 145.3, 142.9, 133.0, 131.5, 130.5, 120.1, and 107.9, three sp^2 methines at δ_C 121.1, 119.4, and 107.2, two sp^3 methylenes at δ_C 25.5 and 21.5, and five methyl carbons at δ_C 25.4, 25.4, 17.8, 17.7, and 11.8 (Table 1).

The UV spectrum was found two peaks with the absorption maxima at 270 and 428 nm indicating the presence of a naphthoquinone chromophore [8, 9]. Analysis of the COSY correlations established the connectivities of H$_2$-10/H-11 and H$_2$-15/H-16. HMBC correlations from the aromatic methine H-5 to C-4a, C-6, C-7, C-8a, the phenolic hydroxy proton 6-OH to C-5, C-6, and C-7, hydrogen-bonded proton 8-OH to C-7, C-8 and C-8a established a pentasubstituted benzene substructure bearing two hydroxy groups. Additionally, H$_3$-9 to C-1, C-2, and C-3, H-5 to C-4, 8-OH to C-1 (four bond correlation, Fig. S5) extended the benzene ring to a 1,4-naphthoquinone core (Fig. 1). The remaining carbons were assigned to constitute two prenyl groups connecting at C-3 and C-7. HMBC correlations from H$_2$-10 and H-11 to C-12, C-13, and C-14, H$_3$-13 to C-11, C-12, and C-14, and H$_3$-14 to C-11, C-12, and C-13 established the carbon-carbon connectivity in a prenyl side chain. The prenyl group was then connected at C-3 by HMBC correlations from H$_2$-10 to C-2, C-3, and C-4. Similarly, another prenyl group was determined to be connected at C-7 (Fig. 2). Two methyl groups of the prenyl groups were distinguished by the ^{13}C chemical shift difference. More shielded methyl resonances at δ_C 17.8 and 17.7 arising from steric compression effect were assigned to C-14 and C-19, respectively.
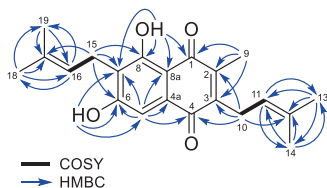
Phytohabimicin (**2**) was isolated as an optically active ([α]$^{22}_D$ + 159 (*c* 0.12, CHCl$_3$)) white powder (2.3 mg from 11 of culture). Its HRESITOFMS spectrum showed deprotonated molecular ions at *m/z* 541.1336, 543.1313, and 545.1296 in a peak area ratio of 9:6:1 (Fig. S16), which inferred the presence of two chlorine atoms in this molecule, thereby establishing the molecular formula C$_{25}$H$_{32}$Cl$_2$N$_2$O$_5$S. The ^{1}H NMR spectrum exhibited two sp^2 methines (δ_H 8.27, 6.81), seven sp^3 methines (δ_H 3.56, 3.13, 3.01, 3.00, 1.66, 1.63, 1.38), six methylenes (δ_H 1.78, 1.65, 1.35, 1.25, 1.22, 0.73), five methyl doublets (δ_H 1.32, 0.95, 0.91, 0.77, 0.75) (Table 2). The ^{13}C and HSQC spectral data confirmed the presence of 25 carbons assignable to one ketone (δ_C 194.2), two carbony-like deshielded carbons (δ_C 177.7, 164.5), four sp^2 carbons (δ_C 147.2, 132.3, 120.9, 111.4), two sp^2 methines (δ_C 128.3, 116.9), one acetal/hemiacetal carbon (δ_C 99.4), two oxygenated sp^3 methines (δ_C 77.3, 75.3), five sp^3 methines (δ_C 43.0, 40.9, 33.9, 32.3, 29.7), three sp^3 methylenes (δ_C 36.7, 33.2, 28.1), and five methyl carbons (δ_C 17.5, 16.9, 13.5, 12.5, 11.5) (Table 2).

COSY analysis clarified three spin systems: a seven-carbon fragment from H$_3$-21 to H$_2$-9 with a methyl substitution at C-7, a six-carbon fragment from H$_3$-23 to H-14 with a methyl group at C-13, and a two-carbon fragment H-15/H$_3$-25 (Fig. 3). These three fragments were joined into one carbon chain from C-5 to C-15 by HMBC correlations from H-6, H$_2$-9, H$_2$-12, and H$_3$-23 to C-10 and H-15 and H$_3$-25 to C-14. Though HMBC correlations that connect C-10 and C-14 were not observed, formation of a 6,6-spiroacetal ring system by the carbons from C-6 to C-14 was inferred by a NOESY correlation between H-6 and H-14 and a deshielded resonance of C-10 (δ_C 99.4), completing an aliphatic part of **2**.

HMBC correlations from the deshielded singlet proton H-3 to C-1, C-2, and C-4 and their ^{13}C chemical shifts

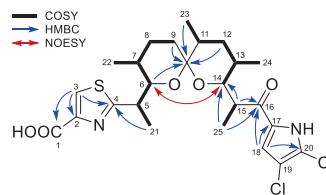**Table 1** NMR data for phytohabinone (**1**) in DMSO-d_6

position	δ_C[a], type	δ_H mult (J in Hz)[b]	HMBC[b,c]
1	188.4, C		
2	142.9, C		
3	145.3, C		
4	183.2, C		
4a	130.5, C		
5	107.2, CH	7.05, s	4, 4a, 6, 7, 8a
6	161.7, C		
7	120.1, C		
8	160.8, C		
8a	107.9, C		
9	11.8, CH$_3$	2.07, s	1, 2, 3
10	25.5, CH$_2$	3.23, d (6.9)	2, 3, 4, 12
11	119.4, CH	4.96, t (6.9)	13, 14
12	133.0, C		
13	25.4, CH$_3$	1.64, s	11, 12, 14
14	17.8, CH$_3$	1.72, s	11, 12, 13
15	21.5, CH$_2$	3.26, d (7.1)	6, 7, 8, 17
16	121.1, CH	5.15, t (7.1)	18, 19
17	131.5, C		
18	25.4, CH$_3$	1.62, s	16, 17, 19
19	17.7, CH$_3$	1.72, s	16, 17, 18
6-OH		11.05, s	5, 6, 7
8-OH		12.64, s	7, 8, 8a

[a]Recorded at 125 MHz (reference δ_C 39.5)

[b]Recorded at 500 MHz (reference δ_H 2.50)

[c]HMBC correlations are from proton(s) stated to the indicated carbon

Fig. 2 COSY and key HMBC for **1**

Table 2 NMR data for phytohabimicin (**2**) in CD$_3$OD

position	δ_C[a], type	δ_H mult (J in Hz)[b]	HMBC[b,c]
1	164.5, C		
2	147.2, C		
3	128.3, CH	8.27, s	1, 2, 4, 5
4	177.7, C		
5	40.9, CH	3.56, dq (7.2, 1.8)	2, 4, 21, 6, 7, 10
6	77.3, CH	3.13, dd (1.8, 10.4)	4, 5, 21, 7, 22, 8, 10
7	32.3, CH	1.38, m	5, 6, 22, 8
8	28.1, CH$_2$	0.73, m; 1.25, m	7, 22, 9, 10
9	33.2, CH$_2$	1.22, m; 1.65, m	7, 8, 10, 11
10	99.4, C		
11	33.9, CH	1.66, m	9, 10, 23, 12, 13
12	36.7, CH$_2$	1.35, m; 1.78, ddd (12.8, 8.5, 4.4)	10, 11, 23, 13, 24, 14
13	29.7, CH	1.63, m	11, 12, 14
14	75.3, CH	3.00, m	13, 24, 15, 25
15	43.0, CH	3.01, m	13, 14, 25, 16, 17
16	194.2, C		
17	132.3, C		
18	116.9, CH	6.81, s	16, 17, 20
19	111.4, C		
20	120.9, C		
21	13.5, CH$_3$	1.32, d (7.2)	5, 6, 7
22	17.5, CH$_3$	0.75, d (6.6)	6, 7, 8
23	16.9, CH$_3$	0.91, d (6.6)	10, 11, 12, 13
24	11.5, CH$_3$	0.95, d (7.0)	12, 13, 14
25	12.5, CH$_3$	0.77, d (6.1)	14, 15, 16

[a]Recorded at 125 MHz (reference δ_C 49.0)

[b]Recorded at 500 MHz (reference δ_H 3.31)

[c]HMBC correlations are from proton(s) stated to the indicated carbon

Fig. 3 COSY and key HMBC and NOESY correlations for **2**

suggested a 2-substituted thiazole-carboxylic acid moiety. The position of the carboxyl group was unable to be assigned only by NMR analysis because thiazole-4-carboxylic acid and thiazole-5-carboxylic acid show almost the same chemical shifts for thiazole carbons and protons (Fig. S15). Bacterial thiazole carboxylic acids are generally synthesized from cysteine by NRPS. The genomic report, BLAST search, and antiSMASH [10] analysis of the closest strain *P. suffuscus* NBRC 105367^T detected a thiazole generating NRPS in a calcimycin-class type I PKS gene cluster. Additionally, thiazole-5-carboxylic acid is not known in natural products (https://dnp.chemnetbase.com). Based on these considerations, the carboxyl group was proposed to be connected at C-2.

The remaining four carbons could be assigned to constitute a pyrrole ring which is commonly present in the structures of calcimycins as a PKS starter unit [11]. Chemical shifts of the carbons from C-17 to C-20 showed close similarity to those for the pyrrole carbons in calcimycins and HMBC correlations shown by an sp^2 methine H-18 to C-16, C-17, and C-20 established the connectivity of this ring system to C-16. Though no HMBC correlation was observed to C-19, the position of this carbon in a pyrrole ring was determined by comparing the reported NMR data

Fig. 4 ^{13}C chemical shift comparison of acyldichloropyrroles
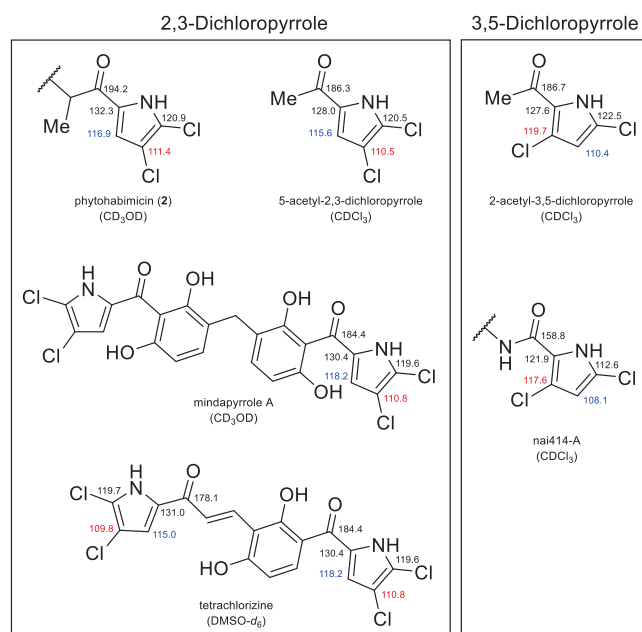
for the related compounds (Fig. 4). The remaining two chlorine atoms were connected to C-19 and C-20 to satisfy the molecular formula. The position of chlorine atoms was further verified by ^{13}C chemical shift comparison with known dichloropyrroles. 2,3 and 3,5-dichloropyrroles show a clear contrast in the ^{13}C chemical shifts of a methine and its neighboring chlorinated carbon: the methine carbons of 5-acetyl-2,3-dichloropyrrole and 2-acetyl-3,5-dichloropyrrole resonates at δ_C 115.6 and 110.4 while the chlorinated C-3 carbons at δ_C 110.5 and 119.7, respectively (Fig. 4) [12]. Several natural products bearing a 2,3-dichloropyrrole show similar chemical shift pattern to **2** [13, 14]. The 3,5-dichloropyrrole moiety in nai414-A shows similar chemical shifts to 2-acetyl-3,5-dichloropyrrole [15]. Finally, these substructures were connected to spiroacetal core structure by HMBC correlations from H$_3$-21 to C-4, COSY fragment H-15/H$_3$-25 to C-14 and C-16 (Fig. 3).

The relative configuration of **2** was determined by analyzing $^3J_{HH}$ coupling constants and NOESY correlation data (Fig. 5). A large vicinal coupling constant between H-6 and H-7 (10.4 Hz) indicated the diaxial orientation of these protons and thus an equatorial orientation of the C-5 substituent. A small coupling constant for H-5 and H-6 (1.8 Hz) together with NOE correlations H-7/H$_3$-21 and H-5/H$_3$-22 allowed the placement of H$_3$-21 methyl group anti to H-6 and H-5 methine directing to the same side as H-7. The anti relationship for H-14/H-15 and H-14/H$_3$-24 were evidenced by a large coupling constant $^3J_{H14,H15}$ 10.2 Hz which was obtained by 1D selective homonuclear decoupling experiment and an NOE correlation H-15/H$_3$-24. Additional NOE correlations H-11/H$_3$-24 and H-13/H$_3$-25 suggested the equatorial orientation of H$_3$-23 and H-13 and the orientation

of H$_3$-25 directing opposite to the C-14 ether oxygen. An NOE between H-6 and H-14 assured the relative configuration of the spiroacetal ring system and these data established the chair conformation of tetrahydropyran rings, thereby establishing the overall relative stereochemistry of **2** as shown in Fig. 5.

The absolute configuration of **2** was analyzed by comparing the experimental and calculated ECD simulation using time-dependent density functional theory (TDDFT). Conformational search using molecular mechanics and subsequent DFT optimization afforded four stable conformers within an energy threshold of 3.0 kcal mol^{-1} (Fig. S13). The calculated spectrum based on those geometries agreed with the experiment ECD of **2** (Fig. 6). The absolute configuration of **2** was thus determined as 5 *R*,6 *S*,7 *S*,10 *R*,11 *R*,13 *R*,14 *S* and 15 *S*, which were identical with that for calcimycin-class metabolites except for the C-7 methyl group. Large chemical shift differences for the carbons C-6, C-7, C-22, and C-8, neighboring C-7, support the inversed configuration of C-7 (Fig. S14).

Biological activities of **1** and **2** were evaluated in antimicrobial, cytotoxicity, and cancer cell migration assays. Antimicrobial activity was tested against Gram-positive and -negative bacteria and yeasts in comparison with calcimycin (Table 3). Compound **1** was weakly active against Gram-positive bacteria while inactive against Gram-negative bacteria and yeasts. Compound **2** showed moderate activity against Gram-positive bacteria, *R. solanacearum*, and yeast while no activity against *E. coli* and *R. radiobacter* (Table 3). Compounds **1**, **2**, and calcimycin exhibited moderate to potent cytotoxic activity against P388 murine leukemia cells with IC$_{50}$ values of 1.7, 4.4, and 0.19 μM, respectively. In
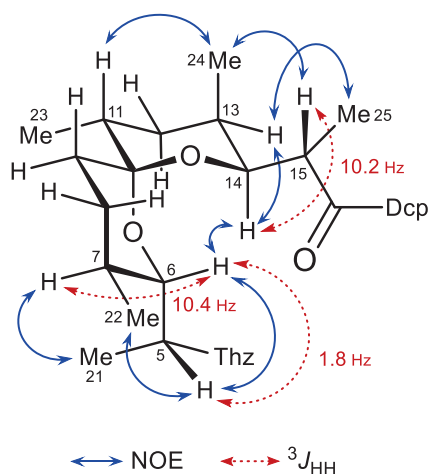
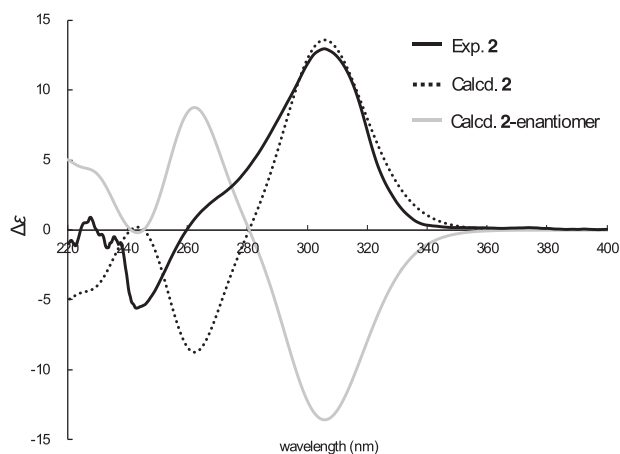**Fig. 5** Relative stereochemical analysis for **2**. Thz thiaxolecarboxilic acid, Dcp dichloropyrrole

Fig. 6 Comparison of the experimental ECD spectrum of **2** in CHCl$_3$ (black line), the calculated ECD spectra of (5 R,6 S,7 S,10 R,11 R,13 R,14 S,15 S)-**2** (dotted line), and its enantiomer (5 S,6 R,7 R,10 S,11 S,13 S,14 R,15 R) (gray line)

Table 3 Antimicrobial activity of compound **1**, **2**, and calcimycin

Microorganisms	MIC (μg ml^{-1})		
	1	**2**	calcimycin
Kocuria rhizophila ATCC 9341	6.3	0.19	0.012
Staphylococcus aureus 209 P JC-1	50	0.19	0.096
Escherichia coli NIH JC-2	>100	>100	>100
Ralstonia solanacearum SUPP1541	>100	6.3	>100
Rhizobium radiobacter NBRC 14554	>100	>100	50
Candida albicans NBRC 0197	>100	0.37	0.078
Saccharomyces cerevisiae S100	>100	0.19	3.1

Fumaquinone is the only reported metabolite in the same prenylated position (Fig. 8).

Compound **2** is a new member of calcimycin-class polyketides. The calcimycin family is characterized by a spiro-oacetal core structure modified with a benzoxazole and pyrrole moieties. Known calcimycin congeners were isolated from *Streptomyces* [17–20], *Dactylosporangium* [21], and *Frankia* [22] and structural variation is seen in the methyl substitution in the polyketide chain and hydroxylation of the benzoxazole (Fig. 8). By contrast, **2** possesses a chlorinated pyrrole and a thiazolecarboxylic acid at both ends of the polyketide backbone and the stereochemically inversed methyl group at C-7 (Fig. 9), which makes this compound distinctive from the previously known calcimycins. These structural differences likely affect the biological activity: calcimycin is inactive against Gram-negative bacterium, *R. sclanacearum*, whereas **2** exhibits moderate activity.

The family *Micromonosporaceae* is one of the most prominent families of actinomycetes. They are recognized as a rich source of various natural products; however, most genera remain unexplored. According to the BLAST search, both *P. suffuscus* and *P. houttuyneae* have an almost complete set of compound **2** biosynthetic genes except for the genes for benzoxazole biosynthesis (Table 4 and S1). In contrast, the calcimycin-producing strain, *Streptomyces chzrteusis* NRRL 3882 lacks halogenase and thiazole biosynthetic genes in its calcimycin cluster. The result suggests that even though core biosynthetic genes are the same, modification genes differ according to the genera. Besides, strain RD003013 shares 100% of 16 S rRNA gene sequences with the strain of *P. suffuscus* K07-0523^T and phytohabitols producing strain RD002984 [7]. Although strain RD003013 produced phytohabitols, strain RD002984 did not produce compounds **1** and **2**; therefore, the ability to produce secondary metabolites is difficult to determine by 16 S rRNA gene similarity. Thus, unstudied rare actinomycetes for natural products are worth detailed screening even though they are the same species in the 16 S rRNA gene. Our recent analysis indicated the high potential of the genus *Phytohabitans* for secondary metabolites. We will report the detail of the metabolite analysis of *Phytohabitans* in the next paper.

addition, **2** significantly inhibited the migration of EC17 cancer cells at 10 μM, which is clearly more effective than the 30 μM positive control, LY294002 (Fig. 7).

Two classes of new polyketides, phytohabinone (**1**) and phytohabimicin (**2**), were discovered from a rare actinomycete *Phytohabitans* sp. RD003013. Compound **1** is a meroterpenoid, mixed with polyketide and terpenoid, which is widely distributed in eukaryotes. Several types of naphthoquinone-based meroterpenoids are known from *Streptomyces* [16] but they were rarely from non-*Streptomyces*. Structurally similar compounds of **1**, phosphatoquinone B [8], fumaquinone [9] (Fig. 7), and other prenylated naphthoquinones were reported from *Streptomyces*; however, prenylation position is different with **1**. The naphthoquinones are prenylated on a quinone ring at C-2 and/or C-3; therefore, one of the prenyltransferases of strain RD003013 seems to be a different lineage.

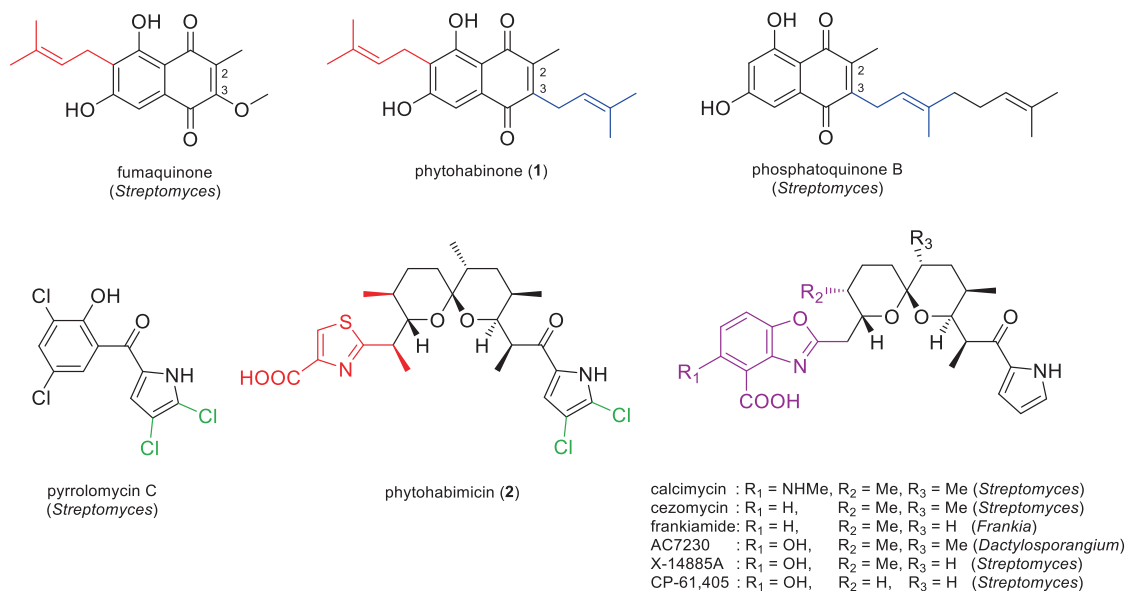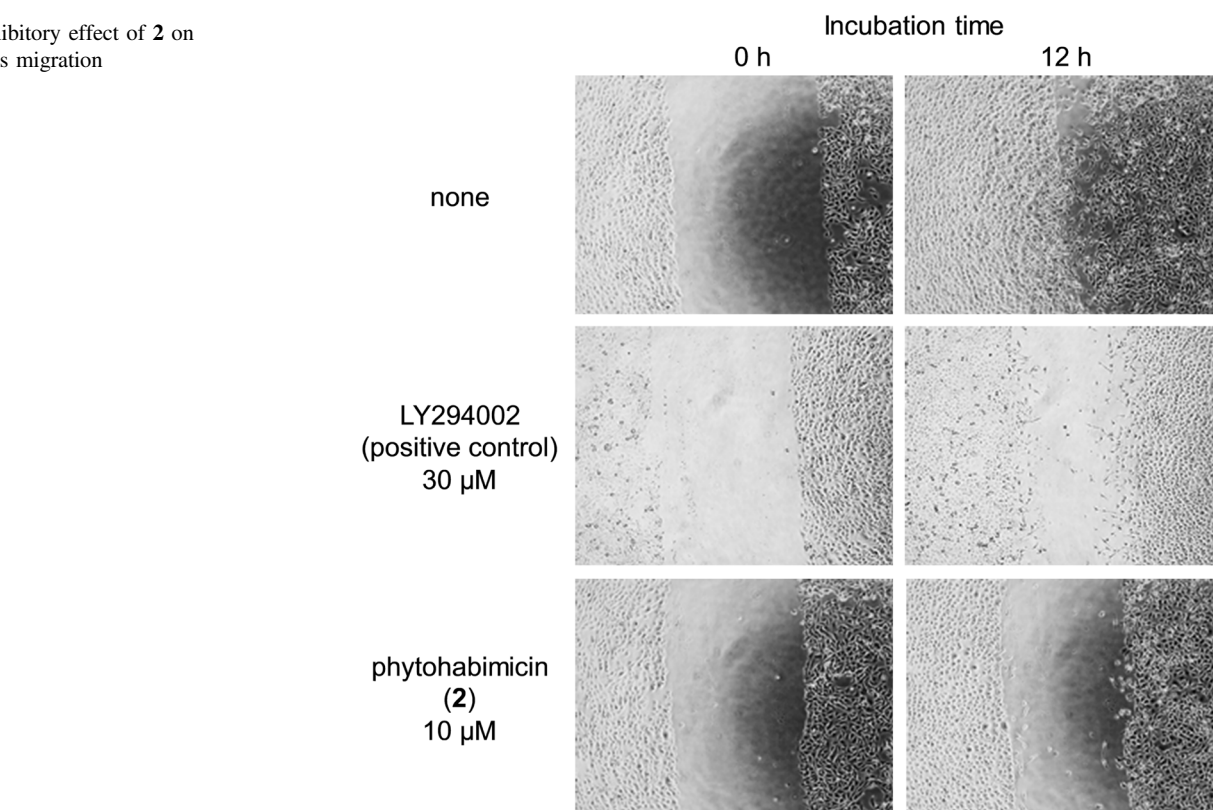**Fig. 7** Inhibitory effect of **2** on EC17 cells migration

Fig. 8 Related natural products of **1** and **2** isolated from actinomycetes

Materials and methods

General experimental procedures

Optical rotations were measured using a DIP-3000 polarimeter (JASCO, Tokyo, Japan). UV spectra were recorded on a UV-1900 spectrophotometer (Shimazu, Kyoto, Japan).

ECD spectra were recorded on a J-720W spectropolarimeter (JASCO). IR spectra were measured by a spectrum 100 spectrometer (PerkinElmer, MA, USA). NMR spectra were obtained on an AVANCE NEO 500 spectrometer (Bruker, MA, USA) in DMSO-d_6 (δ_H 2.50, δ_C 39.5) and CD$_3$OD (δ_H 3.31, δ_C 49.0). HRESITOFMS spectra were recorded on a compact QTOF mass spectrometer (Bruker)

Fig. 9 Putative biosynthetic pathway for phytohabimicin (**2**)
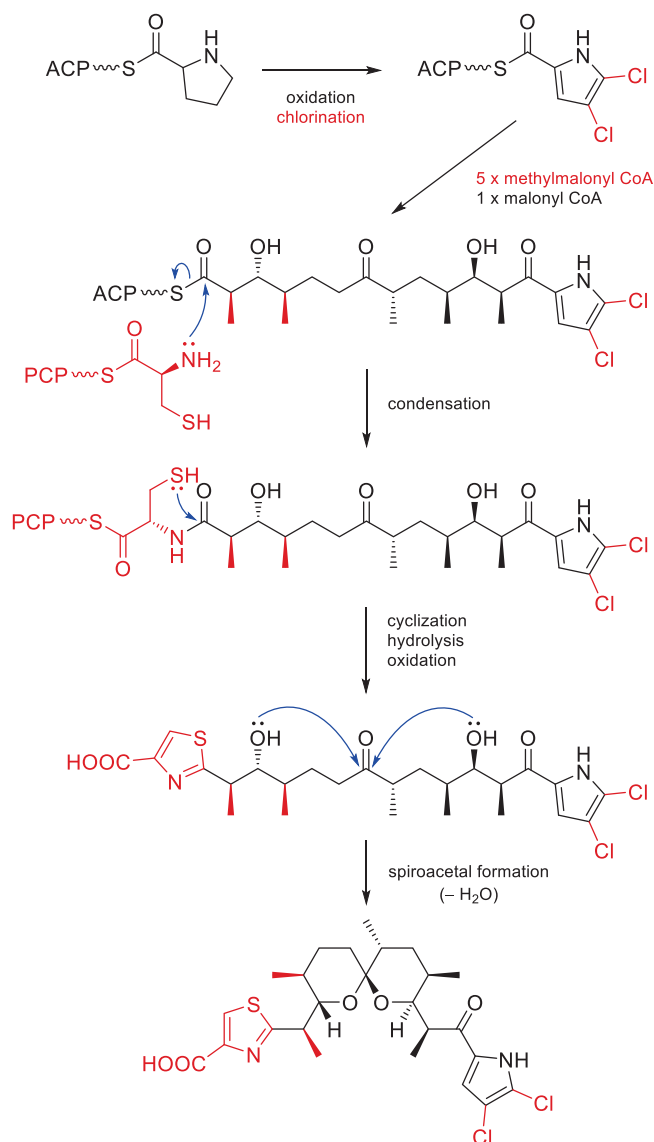
Cosmosil 75C18-PREP (Nacalai Tesque, Inc. Kyoto, Japan) for flash ODS column chromatography. HPLC separations were performed using a COSMOSIL 5C$_{18}$-PAQ Packed Column (10 × 250 mm, Nacalai Tesque, Inc.). The computational study was performed using MacroModel implemented in the Maestro 12.8 software package [23] and the Gaussian16 Rev C.01 program [24]. A part of these computations was conducted using the SuperComputer System, Institute for Chemical Research, Kyoto University. Molecular structures were visualized using the Maestro 12.8 software package. ECD spectra were visualized using GaussView 6.0.16 and Microsoft Excel.

Microorganism

Strain RD003013 was obtained from Biological Resource Center, National Institute of Technology and Evaluation

(NBRC), Chiba, Japan. The results of phylogenetic analysis based on 16 S rRNA gene sequences indicated that strain RD003013 belonged to the genus *Phytohabitans* (Fig. S17). The highest similarity value was observed with *Phytohabitans suffuscus* K07-0523^{T} (AB490769, 100.0%). The DDBJ accession number for the 16 S rRNA gene sequence of strain RD003013 is LC688267 (1425 nucleotides).

Fermentation and isolation

Strain RD003013 growing on an ISP 2 agar medium consisting of 0.4% yeast extract (Kyokuto Pharmaceutical Industrial, Tokyo, Japan), 1.0% malt extract (Becton Dickinson, NJ, USA), 0.4% glucose (pH 7.2) was inoculated into 500-ml K-1 flasks (custom-ordered cylindrical flask) each containing 100 ml of the V-22 seed medium consisting of 1.0% soluble starch, 0.5% glucose, 0.3% N-Z-

Table 4 Blast search of compound **2** biosynthetic gene clusters in *P. suffuscus*

Compound	Query gene		Query cover	Identity	Size (aa)	Accession no.
calcimycin	spiroacetal	A1	62%	58%	1642	WP_232074651.1
		A2	92%	47%	2151	WP_173152420.1
		A3	–	–	–	–
		A4	38%	63%	766	BCB84570.1
		A5	82%	45%	4785	WP_173166170.1
	benzoxazole	B1	–	–	–	–
		B2	–	–	–	–
		B3	–	–	–	–
		B4	–	–	–	–
	pyrrole	N1	79%	44%	381	WP_173155808.1
		N2	99%	65%	491	WP_197945863.1
		N3	90%	60%	86	WP_173155788.1
pyrrolomycin	pyrrole	Pyr7	99%	41%	381	WP_173155808.1
		Pyr8	98%	59%	486	WP_173078670.1
		Pyr28	93%	42%	88	WP_173152388.1
	halogenase	Pyr29	99%	72%	448	WP_173153350.1

case (Wako Pure Chemical Industries, Tokyo, Japan), 0.2% yeast extract, 0.5% Tryptone (Becton Dickinson), 0.1% K_2HPO_4, 0.05% $MgSO_4 \cdot 7H_2O$, and 0.3% $CaCO_3$ in distilled water (pH 7.0). The flasks were placed on a rotary shaker (200 rpm) for 7 days at 30 °C. Then, the seed cultures (3 ml) were transferred to 500-ml K-1 flasks, each containing 100 ml of the A-11M production medium consisting of 2.5% soluble starch, 0.2% glucose, 0.5% N-Z-Amine A (Wako Pure Chemical Industries, Tokyo, Japan), 0.5% yeast extract, 0.3% $CaCO_3$, and 1.0% Diaion HP-20 resin (Mitsubishi Chemical, Tokyo, Japan) in distilled water. The pH of the medium was adjusted to 7.0 before sterilization. All the media were sterilized by autoclaving at 121 °C for 20 min. The inoculated 20 flasks were placed on a rotary shaker (200 rpm) at 30 °C for 14 days. After incubation, 100 ml of 1-BuOH was added to each flask, and the flasks were allowed to shake for 1 h. The mixture was centrifuged at 6000 rpm for 10 min, and the organic layer was separated from the aqueous layer containing the mycelium. The BuOH layer was evaporated to give 11.1 g of extract from 6.3 l of culture. The extract was fractionated using silica gel column chromatography with a step gradient of $CHCl_3$ and MeOH (1:0, 20:1, 10:1, 4:1, 2:1, 1:1, and 0:1 v/v). The fraction 4:1 containing **1** and **2** was concentrated to give 3.0 g, which was subjected to ODS flash column chromatography with a gradient of MeCN and 0.1% HCO_2H solution (2:8, 3:7, 4:6, 5:5, 6:4, 7:3, 8:2, and MeOH v/v), and then washed with MeOH. The washing fraction was evaporated, and the remaining aqueous layer was extracted three times with EtOAc and concentrated to give a red solid (974.6 mg). 314 mg of the fraction was

subjected to ODS flash column chromatography with a gradient of MeCN/0.1% HCO_2H solution (5:5, 6:4, 7:3, 8:2, 8:2, 8:2, 8:2, 8:2, 8:2, 9:1, 9:1, 9:1, 9:1, 9:1, and 9:1 v/v), and then washed with MeOH. The third fraction of 9:1 was evaporated, and the remaining aqueous layer was extracted three times with EtOAc and concentrated to give a red solid (17.9 mg). The final purification was achieved by preparative HPLC using an isocratic condition of 66% MeCN/ 0.1% HCO_2H solution at 4 ml min^{-1}, yielding **1** (5.5 mg) and **2** (6.0 mg) with a retention time of 21.0 min and 17.9 min, respectively.

Phytohabinone (**1**): yellow amorphous solid; UV (MeOH) λ_{max} (log ε) 270 (4.23), 428 (3.62); IR (ATR) ν_{max} 3392, 2912, 1624, 1588, 1442, 1329, 1226, 1055, 795 cm^{-1}; ^{1}H and ^{13}C NMR data, Table 1 and Supporting Information; HRESI-TOFMS *m/z* 339.1600 [M − H]$^{-}$ (calcd for $C_{21}H_{23}O_4$, 339.1602).

Phytohabimicin (**2**): white powder; $[\alpha]^{22}_{D}$ + 159 (*c* 0.12, $CHCl_3$); UV (MeOH) λ_{max} (log ε) 238 (3.40), 296 (3.55); ECD (9.2 × 10^{-5} M, $CHCl_3$) λ_{max} ($\Delta\varepsilon$) 305.6 (+13.0), 242.8 (−5.6) nm; IR (ATR) ν_{max} 2932, 1650, 1401, 1083, 987 cm^{-1}; ^{1}H and ^{13}C NMR data, Table 1 and Supporting Information; HRESI TOFMS *m/z* 541.1336 [M − H]$^{-}$ (calcd for $C_{25}H_{31}{}^{35}Cl_2N_2O_5S$, 541.1336).

Computational analysis

The conformational sampling of structure **2** was performed by applying 100,000 steps of the Monte Carlo Multiple Minimum (MCMM) method with PRCG energy minimization by the OPLS4 force field to obtain 124

conformational isomers within 10.0 kcal mol^{-1} from the minimum energy conformer. Geometries of the conformers were then optimized at the M06-2X/6-31 G(d) level of theory with the SMD solvation model (CHCl$_3$). Frequency calculations were carried out at the same level of theory to confirm the absence of imaginary frequencies and obtain thermal corrections for the Gibbs free energy. After eliminating duplicated structures with the threshold of 0.01 Å RMSD, the single-point energy was calculated at the M06-2X/def2-TZVP-SMD(CHCl$_3$) level of theory, affording four conformers within 3.0 kcal mol^{-1} from the minimum Gibbs free energy. The ECD spectrum of each conformer was simulated by the TDDFT calculation of 25 excited states at the ωB97X-D/def2-TZVP-IEFPCM(CHCl$_3$) level of theory. The spectrum of **2** was created by the weighted average of the above-obtained spectra (half-width: 0.24 eV) according to the Boltzmann distribution, applied the UV correction, and scaled the vertical axis.

Biological assays

Antimicrobial, cytotoxicity, and cell migration assays were carried out according to the method described previously [25, 26].

Compliance with ethical standards

Conflict of interest The authors declare no competing interests.

References

1. Saito S, Indo K, Oku N, Komaki H, Kawasaki M, Igarashi Y. Unsaturated fatty acids and a prenylated tryptophan derivative from a rare actinomycete of the genus *Couchioplanes*. Beilstein J Org Chem. 2021;17:2939–49.

2. Lu S, Harunari E, Oku N, Igarashi Y. Trehangelin E, A bisacyl trehalose with plant growth promoting activity from a rare actinomycete *Polymorphospora* sp. RD064483. J Antibiot. 2022;75:296–300.

3. Saito S, Oku N, Igarashi Y. Mycetoindole. An N-acyl dehydrotryptophan with plant growth inhibitory activity from an actinomycete of the genus *Actinomycetospora*. J Antibiot. 2022;75:44–7.

4. Inahashi Y, Matsumoto A, Danbara H, Omura S, Takahashi Y. *Phytohabitans suffuscus* gen. nov., sp. nov., an actinomycete of the family *Micromonosporaceae* isolated from plant roots. Int J Syst Evol Microbiol. 2010;60:2652–8.

5. Uchida R, Yokota S, Matsuda D, Matsumoto A, Iwamoto S, Onodera H, Takahashi Y, Tomoda H. Habiterpenol, a novel abrogator of bleomycin-induced G2 arrest in Jurkat cells, produced by *Phytohabitans suffuscus* 3787-5. J Antibiot. 2014;67:777–81.

6. Komaki H, Tamura T. Polyketide synthase and nonribosomal peptide synthetase gene clusters in type strains of the genus *Phytohabitans*. Life. 2020;10:257.

7. Saito S, Xiaohanyao Y, Zhou T, Nakajima-Shimada J, Tashiro E, Triningsih DW, Harunari E, Oku N, Igarashi Y. Phytohabitols A–C, δ-lactone-terminated polyketides from an actinomycete of the genus *Phytohabitans*. J Nat Prod. 2022;85:1697–703. https://doi.org/10.1021/acs.jnatprod.2c00137.

8. Kagamizono T, Hamaguchi T, Ando T, Sugawara K, Adachi T, Osada H. Phosphatoquinones A and B, novel tyrosine phosphatase inhibitors produced by *Streptomyces* sp. J Antibiot. 1999;52:75–80.

9. Charan RD, Schlingmann G, Bernan VS, Feng X, Carter GT. Fumaquinone, a new prenylated naphthoquinone from *Streptomyces fumanus*. J Antibiot. 2005;58:271–4.

10. Blin K, Shaw S, Kloosterman AM, Charlop-Powers Z, van Wezel GP, Medema MH, Weber T. AntiSMASH 6.0: Improving cluster detection and comparison capabilities. Nucleic Acids Res. 2021;49:W29–W35.

11. Wu Q, Liang J, Lin S, Zhou X, Bai L, Deng Z, Wang Z. Characterization of the biosynthesis gene cluster for the pyrrole polyether antibiotic calcimycin (A23187) in *Streptomyces chartreusis* NRRL 3882. Antimicrob Agents Chemother. 2011;55:974–82.

12. Duran-Sampedro G, Agarrabeitia AR, Garcia-Moreno I, Costela A, Bañuelos J, Arbeloa T, López Arbeloa I, Chiara JL, Ortiz MJ. Chlorinated BODIPYs: surprisingly efficient and highly photostable laser dyes. Eur J Org Chem. 2012;2012:6335–50.

13. Lacerna NM, Miller BW, Lim AL, Tun JO, Robes J, Cleofas M, Lin Z, Salvador-Reyes LA, Haygood MG, Schmidt EW, Concepcion GP. Mindapyrroles A-C, Pyoluteorin analogues from a shipworm-associated bacterium. J Nat Prod. 2019;82:1024–8.

14. Purdy TN, Kim MC, Cullum R, Fenical W, Moore BS. Discovery and biosynthesis of tetrachlorizine reveals enzymatic benzylic dehydrogenation via an ortho-quinone methide. J Am Chem Soc. 2021;143:3682–6.

15. Mazzetti C, Ornaghi M, Gaspari E, Parapini S, Maffioli S, Sosio M, Donadio S. Halogenated spirotetronates from *Actinoallomurus*. J Nat Prod. 2012;75:1044–50.

16. Murray LAM, Mckinnie SMK, Moore BS, George JH. Meroterpenoid natural products from *Streptomyces* bacteria-the evolution of chemoenzymatic syntheses. Nat Prod Rep. 2020;37:1334–66.

17. Chaney MO, Demarco PV, Jones ND, Occolowitz JL. The Structure of A23187, a divalent cation ionophore. J Am Chem Soc. 1974;96:1932–3.

18. David L, Kergomard A. Production by controlled biosynthesis of a novel ionophore antibiotic, cezomycin (demethylamino a23187). J Antibiot. 1982;35:1409–11.

19. Liu CM, Chin M, Prosser BL, Palleroni NJ, Westley JW, Miller PA. X-14885A, a novel divalent cation ionophore produced by a *streptomyces* culture: discovery, fermentation, biological as well as ionophore properties and taxonomy of the producing culture. J Antibiot. 1983;36:1118–22.

20. Cullen WP, Celmer WD, Chappel LR, Huang LH, Jefferson MT, Ishiguro M, Maeda H, Nishiyama S, Oscarson JR, Shibakawa R, Tone J. CP-61,405, a novel polycyclic pyrrolether antibiotic produced by *Streptomyces routienii* Huang sp. nov. J Ind Microbiol. 1988;2:349–57.

21. Yaginuma S, Awata M, Muto N, Kinoshita K, Mizuno K. A novel polyether antibiotic, AC7230 (3-hydroxycezomycin or its stereoisomer). J Antibiot. 1987;40:239–41.

22. Klika KD, Haansuu JP, Ovcharenko VV, Haahtela KK, Vuorela PM, Sillanpää R. Frankiamide: a structural revision to demethyl (C-11) cezomycin. Z fur Naturforsch-Sect B J Chem Sci. 2003;58:1210–15.

23. MacroModel, Schrödinger, LLC: New York, NY, 2020.

24. Gaussian 16, Revision C.01; Gaussian, Inc.: Wallingford, CT, 2016.

25. Nakae K, Yoshimoto Y, Sawa T, Homma Y, Hamada M, Takeuchi T, Imoto M. Migrastatin, a new inhibitor of tumor cell migration from *Streptomyces* sp. MK929-43F1. Taxonomy, fermentation, isolation and biological activities. J Antibiot. 2000;53:1130–6.

26. Sharma AR, Harunari E, Oku N, Matsuura N, Trianto A, Igarashi Y. Two antibacterial and PPARα/γ-agonistic unsaturated keto fatty acids from a coral-associated actinomycete of the genus *Micrococcus*. Beilstein J Org Chem. 2020;16:297–304.